Journal of Thermal Analysis, Vol.41 (1994) 701-712

In celebration of the 60th birthday of Dr. Andrew K.Galwey

TG AND DSC INVESTIGATION OF THE DEHYDRATION OF THE EXTRA LARGE PORE ALUMINOPHOSPHATE MOLECULAR SIEVE VPI-5 AND RELATED MATERIALS

E. Segal[1], L. Maistriau[2], E. G. Derouane[2] and Z. Gabelica[2]*

[1]University of Bucharest, Faculty of Chemistry, Department of Physical Chemistry, Bulevardul Republicii, 13 Bucharest, Romania

[2]Facultes Universitaires N.D. de la Paix, Laboratoire de Catalyse, 61 Rue de Bruxelles, B-5000 Namur, Belgium

Abstract

The dehydration of a series of VPI-5 and H3 samples, synthesized under various conditions, as well as the solid state transformation of VPI-5 to $AlPO_4$-8 have been investigated using combined TG-DTG-DSC and high-resolution solid state ^{31}P-NMR.The TG curves show a quasi-continuous release of water, the total loss being characteristic for each sample. Complete dehydration is achieved when the samples are heated from 20°C to about 150°C at various heating rates. Besides the main dehydration effect, several weak endothermic peaks are observed. These generally non-reproducible modulated peaks, recorded at high heating rates, are presumably due to the interactions of the water molecules leaving the channels of VPI-5 with the randomly positioned fragments stemming from the destruction of the water triple helix assemblage.

The non-isothermal kinetic parameters of the dehydration have been evaluated from the TG and DTG curves recorded at low heating rates.

Keywords: dehydration, extra-large pore aluminophosphate, kinetics, TG-DTG-DTA

Introduction

The synthesis and general characterization of the extra-large pore (silico)aluminophosphate VPI-5 is widely reported in the recent literature [1-15]. Some properties such as thermal stability of these materials with respect to the water release [1, 16] or their solid state transformation to $AlPO_4$-8 [5, 15-19] have received particular attention.We have analyzed the influence of the

* To whom correspondence should be addressed.

John Wiley & Sons, Limited, Chichester
Akadémiai Kiadó, Budapest

synthesis conditions and of some specific post-synthesis treatments on the stability of VPI-5 [20, 21].

This paper reports a more detailed study of the dehydration of the VPI-5 samples, synthesized under various conditions, and of some related materials, such as H3, that often co-crystallize with VPI-5, with the aim of determinating the conditions under which the transformation from VPI-5 to $AlPO_4$-8 occurs, and the possible influence of the H3 traces on such a transformation.

Experimental

Synthesis

Sample A was prepared from a biphasic medium having the following molar composition: 1 Al_2O_3 : 0.9 P_2O_5 : 0.4 SiO_2 :0.9 DPA : 33.4 H_2O : 5.4 hexanol. Alumina (Catapal-B) was added slowly with stirring to the phosphoric acid solution (H_3PO_4, 85 wt. %) to prepare a homogenous $AlPO_4$ mixture. This mixture was then aged for 3 h at 20°C before the addition of di-*n*-propylamine (DPA). After another 2 h of ageing at 20°C, the organic phase (hexanol), containing the silicon source (tetraethylorthosilicate), was added. The biphasic system obtained was further aged for 2 h and was left to crystallize in autoclave at 125°C for 16 h. The final crytalline product was washed several times with cold water and dried overnight at ambient temperature. It exhibits the VFI structure, but contains small amounts of H3 (XRD data).

Sample B was obtained from a gel having the same molar composition, except that no silicon and hexanol were added. The order of mixing of reactants, the crystallization time and temperature were identical. The final crystallization product was a pure 100% crystalline VFI structure (XRD).

Samples C and D were prepared by following a procedure derived from conditions described in reference [1]: 150 g of alumina (Catapal-b) were slurried in 435 g of demineralized water, to which a solution of 237 g of H_3PO_4 (85 wt. %) in 218 g of demineralized water was added with stirring. The mixture was aged for 3 h before the addition of 7.7 g of SiO_2 (Degussa Aerosil 200) and 109 g of DPA. The resulting gel was aged for 2 h and then left to crystallize at 130°C in the autoclave for 18 h (Sample C), and at 125°C for 16 h (Sample D). The final crystalline product C (VPI-5) contains small amounts of H3, while sample D is pure VPI-5 (with traces of an amorphous phase).

Sample E was prepared from a gel having the following molar composition: 1 Al_2O_3 : 0.5 P_2O_5: 0.9 SiO_2 : 0.9 DPA : 40 H_2O. The order of mixing of the reactants was identical to the one used for samples C and D. After 16 h of crystal-

lization at 125°C, the crystalline product was identified by XRD as pure H3 phase.

The codes used to identify the products synthesized according to the above-mentioned conditions, as well as the nature of the as-synthesized materials (hydrated) and of the same dehydrated materials (after the TG-DSC treatments – see later) are given in Table 1.

Table 1 Nature, percentage and crystallinity (XRD) of the as-synthesized materials as well as of the corresponding dehydrated phases

Samples	As-synthesized materials	Dehydrated materials
A	VPI–5 (95) + H3 (5)	VPI–5 + H3
B	VPI–5 (100)	$AlPO_4$ – 8
C	VPI–5 (90) + H3 (10)	$AlPO_4$ – 8 + H3
D	VPI–5 (85) + amorphous	$AlPO_4$ – 8 + amorphous
E	H3 (100)	H3

Characterization

The nature of the products was determined by X-Ray powder Diffraction (XRD) using a Philips PW 1349/30 diffractometer (CuK_α radiation). The mean size of the crystallites have been evaluated on the basis of the diffractograms recorded, using the formula proposed by Scherrer [22, 23]. The NMR spectra were obtained on a Bruker MSL 400 spectrometer operating at field of 9.39 T. The detailed conditions are given elsewhere [20].

Thermal analysis

Thermal analysis measurements were performed using SETARAM TG-DSC 111equipment. Samples were heated (TG, DTG, DSC) in the temperature range 20–200°C at various heating rates (1 deg·min^{-1} to 10 deg·min^{-1}) under helium flow. Kinetic parameters were determined from TG curves, corresponding to a single step dehydration in the investigated temperature range.Three integral methods described by Coats and Redfern [24], by Flynn and Wall for constant heating rate [25], and by Urbanovici and Segal (a variant of the Coats-Redfern procedure) [26] were applied, using a program written in BASIC language [27].

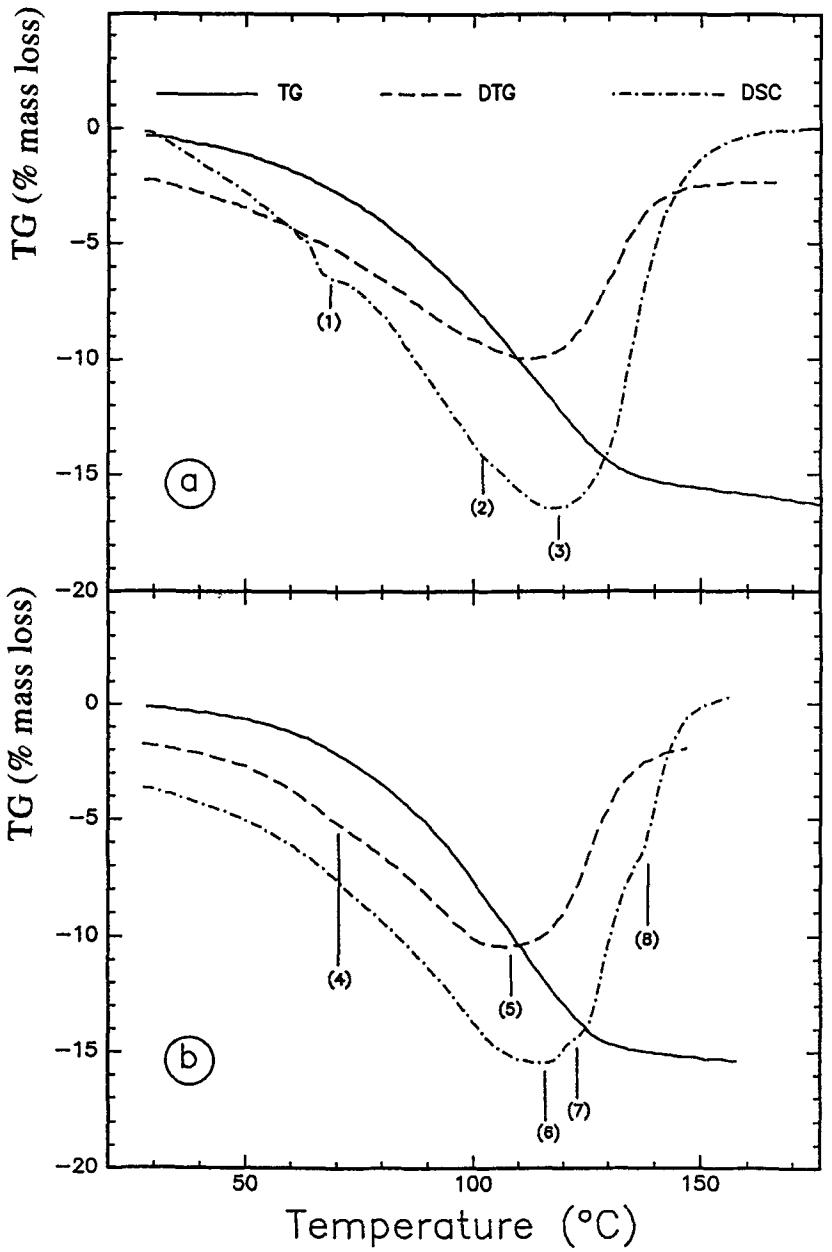

Fig. 1 TG-DTG-DSC curves of compound A heated at 10 deg·min^{-1} under He flow recorded successively for two samples under identical conditions (a) and (b). Peaks and shoulders (1) to (8) as commented in the text

Results

Dehydration of sample A

The TG-DTG-DSC curves recorded at $\beta = 10$ deg·min^{-1} (β = heating rate) are given in Fig. 1a. The TG curve shows a continuous mass loss of 16.6 % (relative to the hydrated material). The shape of the DTG curve confirms the continuous character of the mass loss since it exhibits only one main minimum at 113°C, corresponding to the maximum dehydration rate. The DSC curve is composed of a weak endothermic peak at 68°C, noted (1) on figure, a very weak endothermic shoulder at 103°C (2) and the main endothermic peak at 117°C (3). Upon repeating the heating under identical conditions, the first weak endothermic shoulder is either shifted to a lower temperature (than 68°C) or is totally absent (Fig. 1b). Conversely, the DTG curve exhibits an additional weak minimum at 71°C (4), the main minimum still remaining near 110°C (5). The absence of any endothermic peak at 68°C (DSC) probably reflects the fact that the absorbed heat is spread over a larger temperature range. Note that no endothermic peak at 103°C on the DSC curve could be recorded, while two additional shoulders were observed at 124°C (7) and 137°C (8), next to the main endothermic peak at 117°C (6) (Fig. 1b).

The heating curves recorded at 5 deg·min^{-1} are shown in Fig. 2a. The TG trace again shows a continuous water release. The DTG curve exhibits only one minimum located at 104°C, while a new endothermic peak located at 34°C is seen on the DSC curve. The endothermic shoulders at 76, 118 and 128°C, are now found shifted to lower temperatures, due to the lower heating rate. All these effects show poor reproducibility; indeed a set of heating curves recorded at the same heating rate show only the endothermic peak located near 108°C (Fig. 2b).

Taking into account the shape of the TG, DTG and DSC curves shown in Fig. 2b, which corresponds to dehydration occurring in a single step, we used the (α, T(°C)) data from the TG curve as input data for evaluating the non-isothermal kinetic parameters. The results obtained, based on a "reaction order" model are listed in Table 2. The value of the non-isothermal kinetic parameters calculated by the three different methods are in quite satisfactory agreement. Using the values of the non-isothermal kinetic parameters determined by the Flynn-Wall method, the TG curve was regenerated and compared with the experimental points. As seen from Fig. 3, the experimental points lie practically on the curve, showing the reliability of the approximation used to evaluate the non-isothermal kinetic parameters.

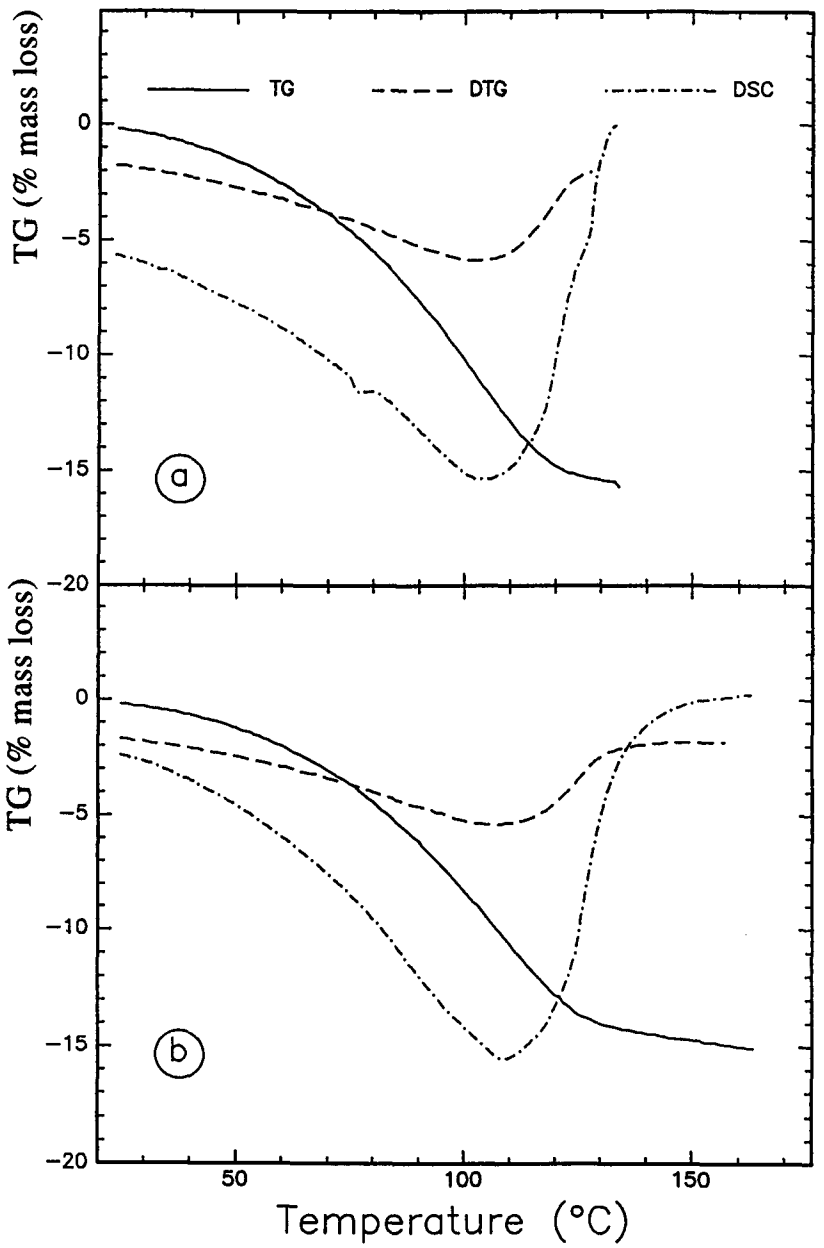

Fig. 2 TG-DTG-DSC curves of compound A heated at 5 deg·min^{-1} under He flow recorded successively for two samples under identical conditions (a) and (b)

Table 2 Values of the non-isothermal kinetic parameters for the dehydration of compound A heated at 5 deg·min^{-1}

Method	Coats-Redfern	Flynn-Wall	Modified Coats-Redfern
n^*	1.6	1.5	1.6
E/kJ·mol^{-1}	52.6	58.3	53.7
A/s^{-1}**	1.1×10^5	3.2×10^5	1.7×105
r***	-0.9963	-0.9971	[0.9962

* n = reaction order, E = activation energy, A = pre-exponential factor

** The values of A are expressed in s^{-1}, as the calculations are based on the rate equation $d\alpha/dt = k(1-\alpha)^n$

*** r is the correlation coefficient of the corresponding linear regression

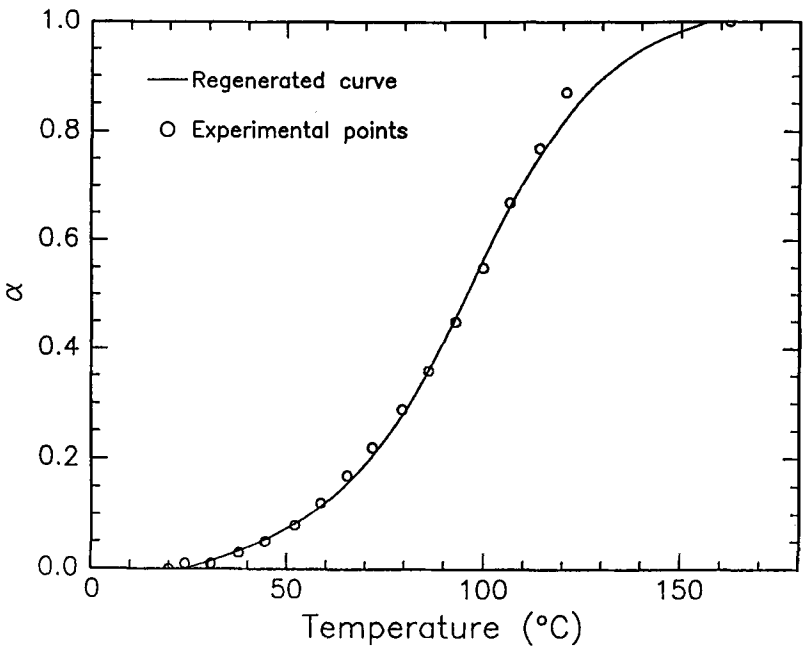

Fig. 3 Regenerated α (degree of conversion) *vs.* T(°C) curve for the dehydration of compound A heated at a rate of 5 deg·min^{-1} using the values of the non-isothermal kinetic parameters obtained by the Flynn-Wall method

Dehydration of samples B, C, D and E

The TG-DTG-DSC curves recorded on heating compounds B, C and D are similar to those of compounds A. Moreover, the shape of the TG curve as well as the location of the main peaks and minima on the DSC and DTG curves are

reproducible, for all the heating rates. However, at high heating rates, i.e. 10 deg·min^{-1}, some additional shoulders are observed on the DTG and DSC curves. Their position is not perfectly reproducible, as already seen in the case of sample A (Fig. 1). When heating rates lower than 10 deg·min^{-1} are used, all the above phenomena are perfectly reproducible.

Table 3 Values of the non-isothermal kinetic parameters for the dehydration of compound D heated at 1 deg·min^{-1}

Method	Coats-Redfern	Flynn-Wall	Modified Coats-Redfern
n	1.3	1.3	1.2
E/kJ·mol^{-1}	54.1	56.8	54.1
A/s^{-1}	1.4×10^{15}	5.4×10^{15}	1.5×1015
r	–0.9976	–0.9980	–0.9974

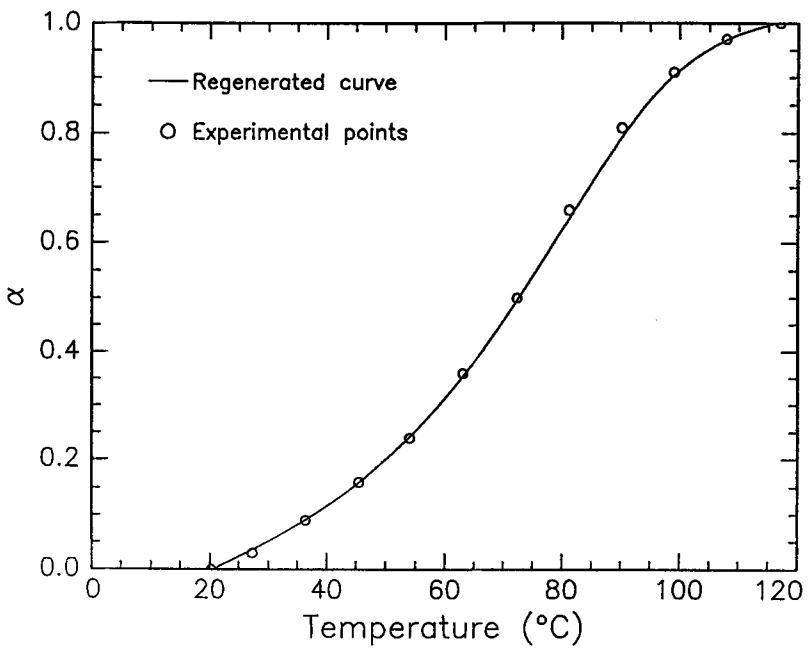

Fig. 4 Regenerated α (degree of conversion) *vs.* T (°C) curve for the dehydration of compound D heated at a rate of 1 deg.min^{-1} using the values of the non-isothermal kinetic parameters obtained by the Coats-Redfern method

When the samples are heated at 1 deg·min^{-1}, besides the main dehydration DSC peak, one can notice a weak endothermic effect in the 30–60 temperature range, probably corresponding to the release of the first water molecule from

the pore volume, as suggested by the corresponding mass loss (TG). Another weak endothermic effect near 110°C possibly corresponds to a phase transition. The single step character of the TG and DTG curves allows the evaluation of the non-isothermal kinetic parameters of the dehydration of sample D. The results are listed in Table 3. The three methods again lead to comparable values for all parameters. The TG curve regenerated using values of the non-isothermal kinetic parameters, determined by the Coats-Redfern method, and the experimental points which fit the same curve, are shown in Fig. 4.

For compound E, the set of heating curves recorded at 10 deg·min^{-1} shows a single continuous dehydration step with a total mass loss of 18.7% at 187°C (relative to the hydrated material). The single main endothermic peak in the DSC curve occurs at 146°C. The same shape of the heating curves is obtained for lower heating rates, except that a series of supplementary endothermic shoulders are recorded at 79 and 81°C (double peak) for a rate of 5 deg·min^{-1} and at 79 and 86°C for a rate of 1 deg·min^{-1}. A weak endothermic phase transition at 172°C without mass loss is recorded, when the sample is heated at 1 deg·min^{-1}.

Table 4 Values of the non-isothermal kinetic parameters for the dehydration of compound E heated at 1 deg·min^{-1}

Method	Coats-Redfern	Flynn-Wall	Modified Coats-Redfern
n	0	0	0
E/kJ·mol^{-1}	39.7	41.4	38.9
A/s^{-1}	4.8×10^{1}	3.7×102	7.6×10^{1}
r	–0.9863	–0.9891	–0.9897

The non-isothermal kinetic parameters of the dehydration are listed in Table 4. The value obtained by applying the three integral methods are in satisfactory agreement.

Discussion

From the above experimental results, the dehydration of all the investigated samples occurs in a continuous or a quasi-continuous way, as shown by the TG curves. The main endothermic peaks (DSC curves) and minima (DTG curves) are satisfactorily reproducible for a given heating rate. Some of the peaks, like the endotherm recorded for low heating rates in the temperature range 30–40°C are characteristic for all the samples except sample E, for which such a peak is extremely weak (if it exists at all).

Rietveld refinement of the VPI-5 structure has suggested a regular arrangement of water molecules within the channels [28]. Seven water molecules are differently positioned in the pore volume of one unit cell: four of them form a H-bonded chain between the octahedrally coordinated framework Al atoms, so as to create a triple helix of H_2O molecules which follows the 6_3 screw axis in the 18 ring channel, and two other H_2O molecules complete the octahedral coordination around the framework Al, located between the fused 4-rings, while the last H_2O molecule, located near the center of the channel, is supposed to link the helices to one another. On this basis, the peak in the range of 30–40°C could be assigned to the release of the water molecules located near the center of the channel [28].

As previously mentioned, besides the main dehydration peaks, some other weak shoulders are irreproducible at high heating rates. These effects can be assigned to the interactions of water molecules with the fragments of the triple helix disposed randomly within the channel system and thus generating irreproducible endothermic peaks at various temperatures, or which various intensities at the same temperature. This irreproducibility of these small endotherms and of the correspondant DTG minima tends to disappear at lower heating rates, e.g. at 1 deg·min^{-1}. Under such conditions, the various endothermic peaks and DTG minima could be assigned to the various interactions of water with the defects in the VFI original lattice, or to defects freshly generated by the collapse of the structure. At this stage, it is difficult to say whether the endothermic phase transition at 110°C is due to the conversion of VPI-5 to $AlPO_4$-8 or to some transformation of lattice defects.

Our data do not account for the existence of a monohydrate VPI-5 type phase as an intermediate of the VPI-5 dehydration [29].

As shown elsewhere [30], the zero value of the reaction order obtained for the dehydration of sample E, corresponds to a reaction limited by the release of water at the outer surface of the crystalline grains. The fractional values of the reaction order, higher than unity, obtained for the dehydration of samples A and D can be assigned to the decomposition of different structural units consisting of variable numbers of molecules, their ratio being characteristic of a given compound. Our results therefore suggest that the dehydration of samples A and D occurs in a kinetic regime.

Conclusions

Some endothermic peaks of the DSC curves and minima on the DTG curves were not reproducible at high heating rates, but were reproducible at low heating rates. The non-reproducible peaks have been assigned to the interaction of

water molecules with the triple helix fragments randomly positioned in the channels of VPI-5. The reproducible peaks have been attributed to the possible interactions of water with the VPI-5 lattice defects.

Except for sample A, all the VPI materials are converted after dehydration to $AlPO_4$-8. In those cases, a phase transition is noticed at 110°C that could possibly account for the transformation of VPI-5 to $AlPO_4$-8.

No correlation between the stability of the VPI structure and the presence of H3 in the as-synthesized material could be established. The stability seems to depend on the synthesis procedure used to crystallize the precursors, directly related to their lattice defect concentrations, thus confirming the results obtained by thermal methods and solid state ^{27}Al- and ^{31}P- NMR [20].

References

1 M. E. Davis, C. Saldarriaga, C. Montes, J. M. Garces and C. Crowder, Nature, 331 (1988) 698.
2 M. E. Davis, C. Montes and J. M. Garces, "Zeolite Synthesis" edited by M. L. Occelli and H. E. Robson (ACS Symp. Series 398, American Chemical Society, Washington D. C., 1989, pp. 291–304.
3 P. J. Grobet, J. A. Martens, J. Balakrishnan, M. Mertens and P. A. Jacobs, Appl. Catal., 56 (1989) L21.
4 S. Prasad and I. Balakrishnan, Inorg. Chem., 29 (1990) 4830.
5 E. G. Derouane, L. Maistriau, N. Dumont, J. B. Nagy and Z. Gabelica, "Synthesis and Properties of New Catalysts: Utilization of Novel Materials Components and Synthesis Techniques" edited by E. W. Corcoran and M. J. Ledoux (Mater. Res. Soc. Proc., Boston, MA, 1990) pp. 3–6.
6 M. E. Davis and D. Young, Stud. Surf. Sci. Catal., 60 (1991) 53.
7 X. Liu and J. Klinowski, "Synthesis and Properties of New Catalysts: Utilization of Novel Materials Components and Synthesis Techniques" edited by E. W. Corcoran and M. J. Ledoux (Mater. Res. Soc./Proc., Boston, MA, 1990), pp. 33–36.
8 J. O. Perez, N. K. Mc Guire and A. Clearfield, Catal. Lett., 8 (1991) 145.
9 H. Cauffriez, Ph. D.Thesis, Mulhouse University, France 1991.
10 L. Maistriau, Z. Gabelica, E. G. Derouane, E.T.C. Vogt and J. van Oene, Zeolites, 11 (1991) 583.
11 E. G. Derouane and R. von Ballmoos, Eur. Patent Appl. No. 146389 (1985).
12 E. G. Derouane, L. Maistriau, Z. Gabelica, A. Tuel, J. B. Nagy and R. von Ballmoos, Appl. Catal., 51 (1989) L13.
13 P. J. Grobet, H. Geerts, J. A. Martens and P. A. Jacobs, Stud. Surf. Sci. Catal., 51 (1989) 193.
14 M. E. Davis, C. Montes and P. E. Hathaway, Zeolites, 9 (1989) 436.
15 L. Maistriau, Z. Gabelica and E. G. Derouane, Appl. Catal., 67 (1991) L11.
16 M. E. Davis, C. Montes, P. E. Hathaway, J. P. Arhancet, D. L. Hasha and J. M. Garces, J. Am. Chem. Soc., 111 (1989) 3919.
17 R. Szostak, B. Duncan, K. Sörby and J. G. Ulan, "Synthesis and Properties of New Catalysts: Utilization of Novel Materials Components and Synthesis Techniques" edited by E. W. Corcoran and M. J. Ledoux (Mater. Res. Soc. Proc., Boston, MA, 1990) pp. 15–17.
18 K. Vinje, J. Ulan, R. Szostak and R. Gronsky, Appl. Catal., 2 (1991) 361.

19 M. Stöcker, D. Akporiaye and K. P. Lillerud, Appl. Catal., 69 (1991) 27.
20 Z. Gabelica, L. Maistriau and E. G.Derouane, "Advances Zeolites and Pillared Clays Synthesis" edited by M. L. Occelli and H. E. Robson, ACS Symp. Series, 1991, pp. 289–315.
21 Z. Gabelica, L. Maistriau and E. G. Derouane, Appl. Catal., 81 (1992) 67.
22 P. Scherrer, Goett. Nachr., 2 (1918) 98.
23 Z. K. Jelinek, "Particle Size Analysis", Malsted Press, 1974, pp. 53–57.
24 A. W. Coats and J. P. Redfern, Nature, 201 (1964) 68.
25 J. H. Flynn and L. A. Wall, Polym.Lett., 4 (1966) 323.
26 E. Urbanovici and E. Segal, Thermochim.Acta, 81 (1984) 379.
27 N. Dragoe and E. Segal, Thermochim. Acta, in press.
28 L. B. McCusker, C. Baerlocher, E. Jahn and M. Bülow, Zeolites, 11 (1991) 305.
29 J. A. Martens, H. Geerts, P. J. Grobet and P. A. Jacobs, "Zeolite Microporous Solids: Synthesis, Structur and Reactivity", NATO ASI, vol. 352, series C, edited by E. G. Derouane, F. Lemos, C. Naccache, F. R. Ribeiro, Kluwer Acad. Publ., Dordrecht, 1992, pp. 477–491.
30 E. Segal, in "Festkörperchemie" edited by V. V. Boldyrev and K. Meyer, VEB Deutscher Verlag für Grundstoffindustrie, Leipzig, 1992, pp. 404.

Zusammenfassung — Mittels kombinierter TG-DTG-DSC und hochauflösendem ^{31}P-Feststoff-NMR wurde die Dehydratation einer Reihe von unter verschiedenen Bedingungen hergestellten VPI-5- und H3-Proben sowie die Feststoffumwandlung von VPI-5 in $AlPO_4$-8 untersucht. Die TG-Kurben zeigen eine quasikontinuierliche Freisetzung von Wasser und die vollständige Abgabe, durch die jede Probe gekennzeichnet ist. Eine vollständige Dehydratation wird erreicht, wenn die Proben bei verschiedenen Aufheizgeschwindigkeiten von 20 auf 150°C erhitzt werden. Neben dem Hauptdehydratationseffekt stehen einige bei höheren Aufheizgeschwindigkeiten registrierte schwache endotherme Peaks wahrscheinlich mit der Wechselwirkung zwischen den die VPI-5-Tunnel verlassenden Wassermolekülen und den zufallsweise positionierten Fragmenten in Zusammenhang, die aus der Zerstörung des Wasser-Dreier-Helixaufbaues stammen.
Anhand der bei niedrigen Aufheizgeschwindigkeiten aufgenommenen TG- und DTG-Kurven wurden die nichtisothermen kinetischen Parameter der Dehydratation ermittelt.